Effects of Compatibilizing Agents in Poly(*n*-butyl acrylate)/Poly(methyl methacrylate) Composite Latexes

PRAPASRI RAJATAPITI,[1,2] VICTORIA L. DIMONIE,[1] MOHAMED S. EL-AASSER,[1,3,*] and MENAS S. VRATSANOS[4]

[1] Emulsion Polymers Institute, [2]Material Science and Engineering, and [3]Chemical Engineering Departments, Lehigh University, Bethlehem, Pennsylvania 18015, and [4]Air Products and Chemicals, Inc., Allentown, Pennsylvania 18195

SYNOPSIS

Graft copolymers with poly(n-butyl acrylate) (PBA) backbones and poly(methyl methacrylate) (PMMA) macromonomer side chains are used as compatibilizing agents for PBA/PMMA composite latexes. The composite latexes are prepared by seeded emulsion polymerization of methyl methacrylate (MMA) in the presence of PBA particles. Graft copolymers were already incorporated into the PBA particles prior to using these particles as seed via miniemulsion (*co*)polymerization of n-butyl acrylate (BA) in the presence of the macromonomers. Comparison between size averages of composite and seed particles indicates no secondary nucleation of MMA during seeded emulsion polymerization. Transmission electron microscopy (TEM) observations of composite particles show the dependence of particle morphologies with the amount of macromonomer (i.e., mole ratio of macromonomer to BA and molecular weight of macromonomer) in seed latex. The more uniform coverage with the higher amount of macromonomer suggests that graft copolymers decrease the interfacial tension between core and shell layers in the composite particles. Dynamic mechanical analysis of composite latex films indicates the existence of an interphase region between PBA and PMMA. The dynamic mechanical properties of these films are related to the morphology of the composite particles, the arrangement of phases in the films, and the volume of the interphase polymer.

INTRODUCTION

Composite latexes often possess properties that are different from latexes of the same polymer composition but are prepared by physical blending of the constituent polymer latexes or by emulsion copolymerization of the corresponding monomers. Seeded emulsion polymerization is the most common preparation method for composite latex particles. Unfortunately, this technique may generate particles with a variety of morphologies. The core-shell morphology, where a second-stage polymer totally covers the seed particles, is only an idealized representation based upon the sequential monomer addition. Transition morphologies, such as hemispherical particles, raspberry, sandwich, mushroom, and confetti-like structures, are frequently reported.[1–3] Design and control of latex particle morphology are often crucial in order to meet the end use requirements for these materials.

Many polymerization parameters can affect composite particle morphology.[1–16] Thermodynamic factors determine the stability of the ultimate particle morphology according to the minimum surface free energy. Kinetic factors, however, control whether the particle is going to reach the thermodynamically predicted degree of phase separation. Thermodynamic parameters typically involve the compatibility between the phases in the system (i.e., hydrophilicity of each phase, particle surface polarity, and interfacial tensions). On the other hand, examples of kinetic factors are cross-linking agent, viscosity of the reaction medium, mode of monomer addition, and polymerization temperature.

* To whom correspondence should be addressed.

Journal of Applied Polymer Science, Vol. 63, 205–219 (1997)
 CCC 0021-8995/97/020205-15

Several researchers specifically examined the role of interfacial tensions in particle morphology.[11–16] Originally, Torza and Mason[11] studied three mutually immiscible liquids where one of the liquids was water. Sundberg et al.[12] applied the approach of Torza and Mason[11] to polymer encapsulating oil droplets in a micrometer size range. They proposed that each particular morphology possesses a different value for free energy; the morphology with the lower free energy is the more thermodynamically favored one. Dimonie et al.[13] studied the effect of process variables on the composite latex particle morphology. Finally, Chen et al.[14–16] investigated the applicability of the interfacial tension approach to predict the particle morphology in seeded emulsion polymerizations. They proposed a pathway of particle morphology during seeded emulsion polymerization according to the free energy changes. Their model describes the surface free energy corresponding to the various possible morphologies of the composite latex particles.

In summary, interfacial tension is one of the most important parameters controlling composite particle morphology. Based on the previous thermodynamic analyses,[11–16] a seeded emulsion polymerization system tends to reach the lowest surface free energy state; that is, the one with the minimum total interfacial energy. Both the interfacial tensions between the different polymer phases and the interfacial tensions between each polymer phase and the aqueous medium are the key factors controlling the equilibrium composite particle morphology. Consequently, one may be able to control the composite particle morphology by monitoring these interfacial tensions.

The objective of our research project is to understand the role of the graft copolymers (used as compatibilizing agents) in reducing the interfacial tension between the core and shell phases of the composite particles. The system studied is poly(n-butyl acrylate)/poly(methyl methacrylate) (PBA/PMMA) composite latex. Compatibilizing agents are graft copolymers with PBA backbones and PMMA macromonomer side chains (BA/PMMA macromonomer graft copolymers). A preceding paper[17] already described the miniemulsion (*co*)polymerization of n-butyl acrylate (BA) in the presence of PMMA macromonomers. This process incorporates macromonomer as side chains into the PBA backbones constituting PBA seed particles *in situ* (during the time of the particle preparation). Due to an extremely low water solubility of the macromonomers, the use of miniemulsion polymerization rather than conventional emulsion method is essential for the successful incorporation of the macromonomers into the PBA particles.[17,18] In the seed latexes, hydrophilic PMMA-macromonomer branches of the copolymers partition close to the particle-water interface and lower the interfacial tension between these phases.[17,19] In the composite latexes, we anticipate that the graft copolymers would also reduce the PBA/PMMA interfacial tension. A lower interfacial tension between these two polymer phases would allow better coverage of the core PBA particles by the shell PMMA.

The present paper focuses on the following subjects: (1) the preparation of the PMMA shell by seeded emulsion polymerization of methyl methacrylate (MMA) on the PBA incorporating macromonomer seeds, (2) the morphological characteristics of the composite particles, and (3) the dynamic mechanical properties of films prepared from composite latexes. The particle morphologies are explained in terms of the change in the interfacial tension between PBA and PMMA. The dynamic mechanical data are interpreted in terms of particle morphology, arrangement of phases in the films, and existence of an interphase layer between the core and shell phases.

EXPERIMENTAL

Materials

Seed latexes (PBA homopolymer or BA/PMMA macromonomer copolymers) and PMMA homopolymer latexes were already prepared by miniemulsion homopolymerization of BA or copolymerization of BA in the presence of PMMA-macromonomer.[17] BA and MMA monomers (Aldrich) were purified by passing through a column filled with an inhibitor remover packing (Aldrich). Sodium lauryl sulfate (Henkel), potassium persulfate (Fisher), phosphotungstic acid (Fisher), and ruthenium(III) chloride hydrate (Aldrich) were used with no further purification. Distilled-deionized (DDI) water was used in all experiments.

Latex Preparation

PBA/PMMA composite latexes were prepared starting from PBA seed latexes (PBA homopolymer or BA/PMMA-macromonomer copolymers)[17] with MMA as the second-stage monomer. Seeded emulsion polymerizations were carried out in a

Table I Recipe for Seeded Emulsion Polymerization to Prepare PBA/PMMA Composite Latexes at 70°C

Ingredients	Weight (g)
Seed latex[a]	10,000
MMA monomer	2.000
DDI water	8.000
Sodium lauryl sulfate (SLS), 2.6 m*M*	0.012
Potassium persulfate (KPS), 3 m*M*	0.013

[a] PBA homopolymer or PBA incorporating PMMA macromonomer; solids content approximately = 20 %.[17]

batch mode. Seed polymer/monomer ratio was 1 : 1 (w/w). Table I gives the recipe for the composite latex preparation. Table II provides the compositions of the latexes used in the subsequent experiments.

Seeded emulsion polymerization procedures are as follows:

1. Dissolve an appropriate amount of sodium lauryl sulfate (SLS) surfactant in water to make a 2.6 m*M* concentration.
2. Add 6 mL of the SLS solution to 10 mL seed latex in a 25 mL flask blanketed with a nitrogen atmosphere.
3. Stir the mixture with a magnetic stirrer for 15 min at room temperature.
4. Swell seed latex particles with 2 mL MMA monomer for 30 min with continuous stirring.
5. Place the mixture in a thermostated bath with circulating hot water at 70°C for 10 min.
6. Dissolve a given amount of potassium persulfate (KPS) initiator in water to make a 3 m*M* concentration.
7. Inject 2 mL of the KPS solution into the flask.
8. Carry out polymerization at 70°C for 6 h.

PBA and PMMA homopolymer latexes were prepared by miniemulsion homopolymerization as described in the previous paper.[17] Compositions for PBA/PMMA homopolymer latex blends are also included in Table II.

Characterization and Testing

Particle Size Determination

Capillary hydrodynamic fractionation (CHDF 1100, Matec Applied Science) was used to measure the particle size distributions of latexes. CHDF samples were prepared by diluting the original latexes with water to 2% solids, sonifying

Table II Compositions of PBA/PMMA Composite Latexes and Homopolymer Blends

Sample	Macromonomer in Seed Latex				Composite or Blend		
			Macromonomer/BA ($\times 10^{-2}$)		PBA/PMMA		
Name	M_w (g/mol)	Weight (g)[a]	mol/mol	w/w	mol/mol	w/w	PBA Volume[b]
BM0	—	—	—	—	0.781	1.000	0.530
BM253	5320	0.400	0.049	2.041	0.766	0.980	0.519
BM512	1260	0.247	0.127	1.250	0.772	0.988	0.523
BM536	3640	0.696	0.127	3.605	0.754	0.965	0.512
BM553	5320	1.000	0.127	5.263	0.742	0.950	0.504
BM596	9640	1.740	0.127	9.529	0.713	0.913	0.485
BM1053	5320	2.000	0.267	11.111	0.703	0.900	0.478
Blend 30					0.335	0.30/0.70	0.33
Blend 50		homopolymer blends			0.781	0.50/0.50	0.53
Blend 65					1.451	0.65/0.35	0.68

[a] 20 g total seed polymers.
[b] Fraction based on total polymer volume. Calculation is based on the densities of PBA and PMMA (1.055 and 1.188 g/cm^3, respectively) and of PMMA macromonomers[20] and the weights of all the components in the latexes.

them in a sonifier bath (Commonwealth Scientific) to break up any aggregates, and filtering these latexes through 5 μm pore size filters (Millipore) before injection. Of all the averages obtained from the CHDF, the main peak number average (Main D_n) was chosen to represent the samples because it better portrays the changes in size of the majority of the particles. Three injections were made for each sample, and the numbers were again averaged.

TEM Observation of Composite Particle Morphology

Morphologies of the composite latex particles were studied using the Phillips TEM-400 at 100 kV. All the images were taken at 60,000 magnification. First, the original latexes were diluted with a 2% aqueous solution of phosphotungstic acid (PTA) stain. Second, we place a drop of each dilute latex on a carbon-coated Formvar film deposited on an aluminum grid. Then, for the preferential staining, the samples were also stained by the ruthenium tetroxide (RuO_4) vapor for 30 min. (RuO_4 vapor was generated by the reaction between ruthenium(III) chloride hydrate and a commercial household bleach.) RuO_4 reacts with PBA at a slightly faster rate than with PMMA. Thus, it allows the differentiation between PBA and PMMA regions. (PBA would appear darker in the micrographs.)

Dynamic Mechanical Studies

All specimens, but one derived from the PBA homopolymer latex, were prepared from freeze-dried latexes. (This technique produces finer powders than air-drying.) The dried polymer was formed into the test specimen by compression molding. The molding conditions were as follows: 0.7–0.8 g of material was preheated to 150–180°C for 30 min, cooled down to 80–120°C, and then kept under pressure (approximately 1000 psi) for 15–45 min. (The actual molding conditions varied from sample to sample.) Each specimen has the following dimensions: 30 × 10 × 1 mm^3 (rectangular torsion geometry).

The PBA homopolymer film was air-dried and cut into a circle of 25 mm diameter (parallel plate geometry).

All dynamic mechanical analyses (DMA) were performed on a Rheometrics Dynamic Analyzer (RDA II), which applies a cyclical shear strain to the sample. This instrument measures the sample stress response in the form of the shear storage modulus (G'), shear loss modulus (G''), and the loss tangent ($\tan\delta$, G''/G'). The testing frequency was 1 Hz, and the temperature range was −100 to 180°C. Soak time was 30 s. Data were collected every 2°C near the transition temperatures, and every 5 or 10°C elsewhere.

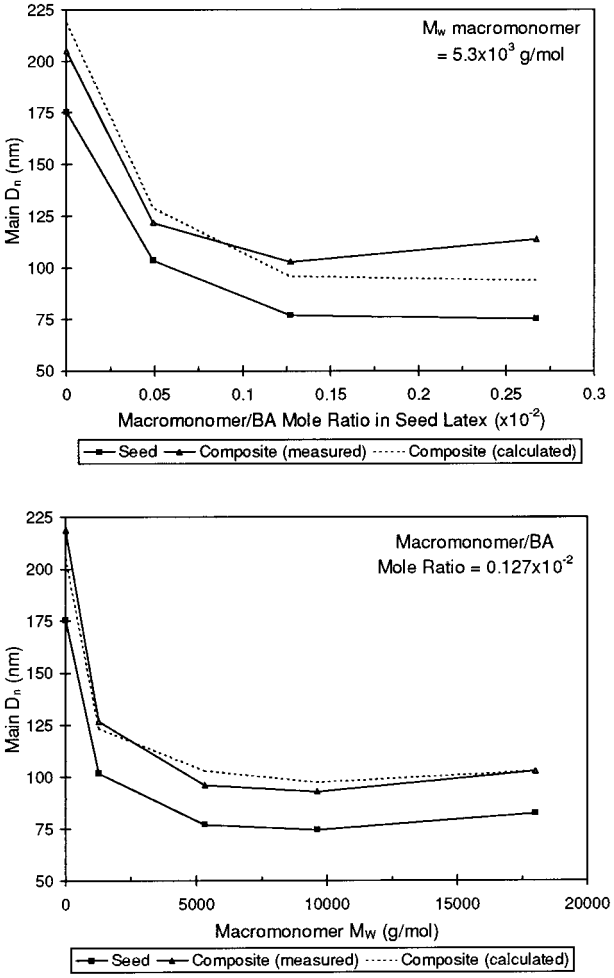

Figure 1 Dependence of the measured particle size averages of seed and composite latex particles on the amount (top) and molecular weight (bottom) of PMMA macromonomers used in the seed latex preparation, and the calculated size of the composite particles.

RESULTS AND DISCUSSION

Latex Particle Size Distributions

Figure 1 shows the dependence of the average sizes of the seed and composite latex particles on the amount (top) and molecular weights (bottom) of macromonomers used in the seed latex preparation. The predicted sizes of the composite particles

Table III Standard Deviations of Size of Composite Latex Particles and Corresponding Seed Particles (CHDF).[a]

Sample Name	Macromonomer in Seed Latex		Standard Deviations (%)			
			Number		Weight	
	M_w (g/mol)	Mole Ratio Based on BA ($\times 10^{-2}$)	Seed	Composite	Seed	Composite
BM0	PBA homopolymer		25	18	41	27
BM253	5320	0.049	41	21	53	26
BM512	1260	0.127	44	36	38	37
BM553	5320	0.127	29	26	37	25
BM596	9640	0.127	53	34	51	32
BM518	18000	0.127	34	28	51	35
BM1053	5320	0.267	47	32	58	43

[a] See Figure 1 for particle size averages.

are also plotted. [The predicted values were calculated based on the average size of the corresponding seed particles[17] and the volume of the second-stage polymer, which was determined from the weight of MMA in the recipe, (Table I), and the density of PMMA (1.188 g/cm^3)]. Table III compares the size distributions of the seed and composite latex particles.

The CHDF data shows that composite particle size averages are larger (Fig. 1), while their size distributions are narrower (Table III) compared with those of the corresponding seed particles. The measured sizes of the composite particles seem to follow the values predicted. (An exception was found for one sample (BM1053). The average size, being larger than expected in this particular case (136 versus 116 nm; Fig. 3), could reflect some particle agglomeration during the second-stage polymerization.) In every sample, no indication of a second-stage nucleation of MMA is observed. These results suggest that MMA was completely polymerized onto the PBA seed particles.

Composite Particle Morphology

This section reports the morphological observations of the composite latex particles. The differences in the particle morphology are explained in terms of the change in the interfacial tension between PBA seed particles and the newly formed PMMA shell, which is dependent on the mole ratio of macromonomer/BA and the molecular weight of the macromonomer used in the seed latex preparation. See Table II for descriptions of these latexes.

Effect of Macromonomer Content

Figure 2 shows TEM micrographs of composite latex particles prepared using (A) PBA homopolymer seed latex (BM0) and (B)–(D) BA/PMMA macromonomer copolymer seed latexes prepared with the same macromonomer ($M_w = 5.3 \times 10^3$ g/mol) but different mole ratios of macromonomer to BA (BM253, BM553, and BM1053).

As seen from the micrographs, the morphologies of composite particles are strongly dependent on the amount of PMMA macromonomer used in the preparation of the seed latexes. The composite particles prepared from PBA homopolymer seed latex (BM0) show a mainly hemispherical morphology, i.e., particles with a light PMMA shell partially covering the dark PBA core [Fig. 2(A)]. This type of morphology is expected because the two polymers are incompatible. Despite their smaller sizes, composite particles prepared from PBA seed incorporating the lowest macromonomer/BA mole ratio [BM253; Fig. 2(B)] has a similar morphology. However, composite latexes prepared from PBA seed incorporating higher amounts of macromonomer (BM553 and BM1053) form particles with a mixture of morphologies. Figures 2(C) and (D) show some large particles with a PMMA-rich surface and smaller particles, which have either hemispherical or multiphase morphology. The uniform core-shell morphology of the larger particles may be attributed to the effect of the BA/PMMA-macromonomer graft copolymers partitioning on the surface of the seed particles. During the second-stage polymerization, the presence of the graft copolymer layer on the surface of these seed particles prevents the newly formed PMMA

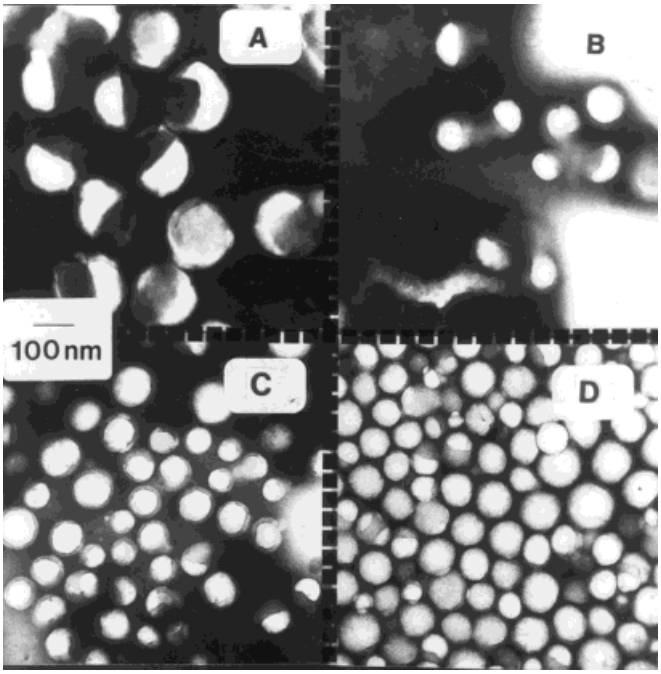

Figure 2 TEM micrographs of PBA/PMMA composite latex particles stained with PTA and RuO_4: (A) BM0, (B) BM253, (C) BM553, and (D) BM1053. Macromonomer $M_w = 5.3 \times 10^3$ g/mol. In these micrographs, PBA is stained dark, whereas PMMA appears light.

from segregating. Thus, PMMA resides on the surface of the particles as a continuous shell. The hemispherical and multiphase particles may result from the inherent composition inhomogeneity of the seed latex. It is possible that, in the miniemulsion polymerization of BA in the presence of macromonomer, some PBA seed particles were formed with little or no graft copolymer on their surfaces. This may be a consequence of either the nonuniform size distribution of the monomer droplets or some homogeneous aqueous phase nucleation of BA during the seed latex preparation.[20]

Effect of Macromonomer Molecular Weight

Figure 3 shows TEM micrographs of a set of samples in which the molecular weight of the macromonomer in the seed latex was varied, while the macromonomer/BA mole ratio was kept constant (0.127×10^{-2}) to maintain a constant number of grafted PMMA chains (BM512, BM553, and BM596). Therefore, the weight ratio of macromonomer to BA was increased with the increasing molecular weight of the macromonomer.

The composite latex particles prepared from PBA seed incorporating low molecular weight macromonomer (BM512) show multiple white domains of second-stage PMMA on the PBA phase [Fig. 3(A)]. Per unit volume, the total interphase area between the two polymer phases in these particles is larger than in those with a hemispherical morphology. This type of morphology suggests that by adding a hydrophilic macromonomer to the seed latex preparation the PBA/PMMA interfacial tension is decreased (to some extent). The lower interfacial tension allows the improved coverage of the seed polymer by the shell PMMA in the composite particles. However, the amount of the graft copolymer in this sample may not be sufficient or its structure does not favor its partitioning at the seed particle surface. Thus, they are not as effective in lowering the interfacial tension between the two polymer phases as when macromonomers of higher molecular weights are used to prepare the seed latexes.

When the higher molecular weight macromonomers are used in the seed latex preparation at the same mole ratio, there are larger numbers of total MMA units and longer PMMA macromonomer grafts in the seed particles (Table II). Both of these lead to a higher concentration of MMA units at the particle interface. Consequently, the interfacial tension is reduced to a lower value. As a result, more uniform coverage of the seed by the

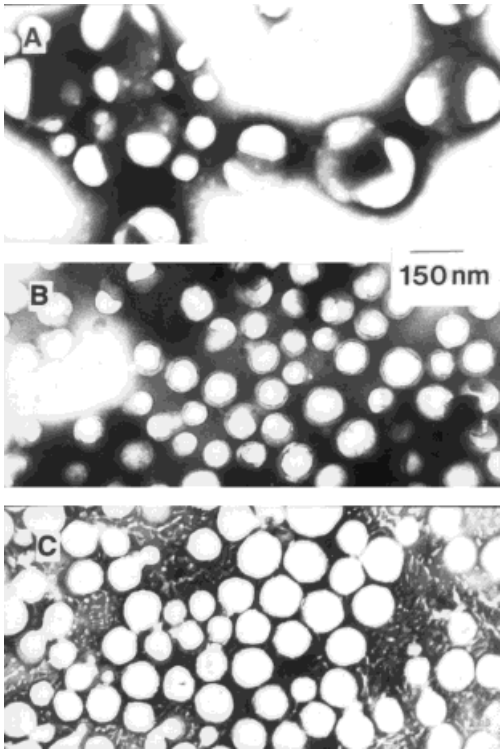

Figure 3 TEM micrographs of PBA/PMMA composite latex particles stained with PTA and RuO_4. Macromonomer/BA mole ratio in seed latex = 0.127×10^{-2}. (A)–(C): BM512, BM553, and BM596. In these micrographs, PBA phase is stained dark by RuO_4, whereas PMMA remains light.

shell polymer is observed. When the PBA seed latex incorporating the macromonomer of the highest molecular weight (BM596) is used as a seed latex, the micrograph exhibits all composite particles with a PBA core completely covered by the PMMA shell [Fig. 3(C)].

Latex Film-forming Abilities at Room Temperature

To observe the latex film formation behavior, two drops of each latex were dried on a microscope glass slide at room temperature. As anticipated from its low T_g (−53°C[21]), the PBA homopolymer formed a clear, sticky, continuous film. In contrast, the PMMA homopolymer latex dried to a white, cracked film because the drying temperature was not high enough for the coalescence of the PMMA particles (T_g = 105°C[21]). A 1 : 1 (w/w) blend of these two homopolymer latexes formed a nonsticky, slightly opaque film. However, although the polymer compositions in the PBA core/PMMA shell latexes are similar to that of the 1 : 1 blend (see Table II), most of these latexes could not form continuous films under these conditions.

The following reasons explained the differences between the film-forming properties of the blend and the composite latexes. (1) In the blend, PBA particles are highly mobile. Thus, they randomly came into contact with each other during the drying process, coalesced, and formed a continuous matrix, while PMMA particles remained dispersed in the matrix. (The slight opacity of the film is likely resulting from the aggregation of PMMA particles to make up domains large enough to scatter light.[22–24]). (2) In the composite latexes, the mobility of the PBA phase is reduced because of its attachment to the PMMA shell of the particles. (Figs. 2 and 3 show the attachment of PBA and PMMA phases in composite latex particles.)

The only composite latex able to form a film is the one prepared from the PBA seed latex particles incorporating the lower molecular weight macromonomer (BM512). This sample possesses a unique particle morphology. For this particular latex, we observed earlier by TEM that a large area of the PBA seed particles was not covered by the small PMMA "lumps" [Fig. 3(A)]. As a result, the exposed PBA phases from neighboring particles can coalesce and form a film. Therefore, this film consists of a PBA matrix and PMMA fillers, similar to the one dried from the PBA/PMMA latex blend.

Polymer Compatibility Studies (DMA)

Previous studies already showed that films derived from PBA/PMMA composite latexes may possess different dynamic mechanical properties, in spite of the same composition, if their particle morphologies are different.[24–27] In the following studies, properties of films from the following latex systems are compared: (1) PBA and PMMA homopolymer latexes, (2) PBA/PMMA homopolymer latex blends, and (3) composite PBA/PMMA latexes prepared using PBA seed particles (PBA homopolymer or BA/PMMA-macromonomer copolymers[17]). See Table II for details of these samples.

PBA/PMMA Homopolymer Latex Blends

The purpose of the following experiment is to determine the arrangement of phases in the mold-compressed polymer films by comparing our experimental data on the blends to the existing data

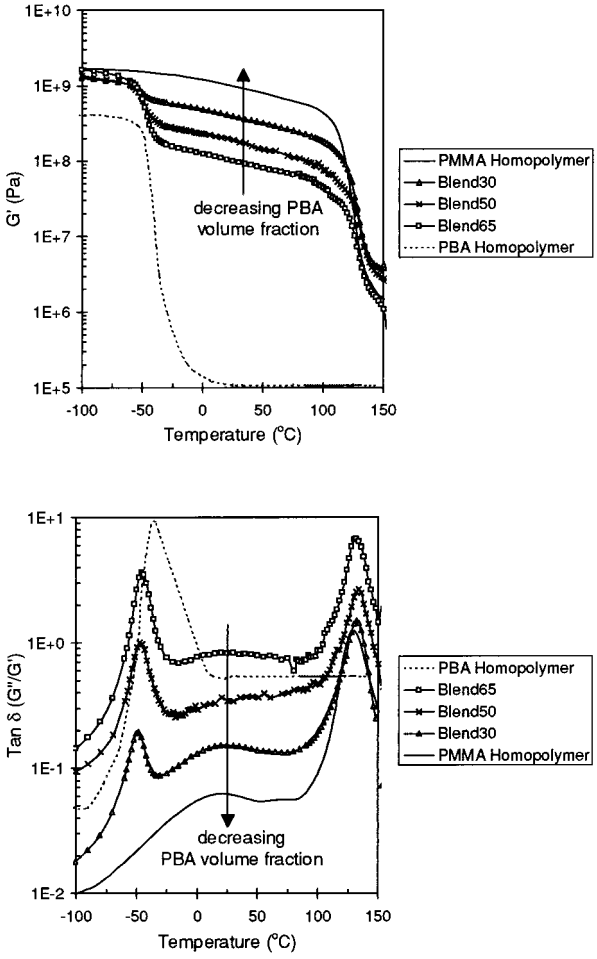

Figure 4 Temperature dependence of G' (top) and tan δ (bottom) for PBA and PMMA homopolymers and PBA/PMMA homopolymer latex blends of different compositions. (See Table II for polymer compositions in the blends.)

for a similar system. Previously, Dickie and coworkers[24–26] studied homopolymer latex blends and composite latexes of 95/5 (mol/mol) PBA/1,3-butylene dimethylacrylate (BDMA) copolymer, P(BA-*co*-BDMA), and PMMA. Their experimental data showed that (1) both the values of G' in the region between the transitions of the constituent polymers and the height of the dispersed phase tan δ peaks in the blends are highly dependent on the volume fraction of the dispersed phase, and (2) the blends' G' curves in the region between the two T_g's are parallel to that of the polymer constituting the continuous phase.

Figure 4 shows the G' (top) and tan δ (bottom) versus temperature curves of the PBA/PMMA blends and those of PBA and PMMA homopolymers. The G' transitions and the tan δ peak positions of the blends correspond well with the T_g's of the homopolymer phases. The slope of the G' curves between the two T_g's are all parallel to that of the PMMA homopolymer. The G' values in this region are higher in blends with lower PBA contents. Moreover, the height of the PBA tan δ peak increases with PBA content of the blend, while the height of the PMMA peak is less affected.

Based on Dickie's conclusions,[24–26] the DMA data suggest that these films consist of PBA domains dispersed in a continuous PMMA matrix. This phase arrangement is possible because during the compression molding process to prepare the DMA specimens, in which the temperature of the mold was raised to 180°C, the PMMA particles in the blend are mobile. Thus, they can coalesce and form a continuous film, trapping PBA particles as dispersed domains. Accordingly, the morphology of the mold-compressed films is different from that of the air-dried films, which are composed of a PBA matrix with PMMA fillers (as seen from the film formation results). (Phase rearrangement upon mechanical or heat treatment of composite latex films is common.)[23,28,29]

Dickie's Model

Based on a comparison between the measured dynamic mechanical properties and the corresponding parameters calculated from a suitable model, DMA is capable of providing information on the film morphology. In the case of films prepared from composite latexes, the film morphology is dependent on the characteristics of the composite particles. Thus, DMA results can also be related to the particle morphology.

The subsequent experiment is designed to establish the validity of the model developed by Dickie and coworkers[24–26] in interpreting our experimental data. This model predicts the modulus of systems, consisting of simple domains perfectly bonded to the continuous matrix based on the following expressions.

$$\frac{G^*}{G_m^*} = \frac{(1 - \phi\nu)G_m^* + (\alpha + \phi\nu)G_i^*}{(1 + \alpha\phi\nu)G_m^* + \alpha(1 - \phi\nu)G_i^*} \quad (1)$$

$$\phi = 1 + \nu(1 - \nu_m)/\nu_m^2 \quad (2)$$

$$\alpha = 2(4 - 5\upsilon_m)/(7 - 5\upsilon_m) \quad (3)$$

where G^* is the complex modulus ($G^* = G' + iG''$); ν is the volume fraction of the dispersed phase; ϕ is an interaction parameter in the form

Table IV Parameters Used in the Calculation of the Moduli and Loss Tangent of the PBA/PMMA Homopolymer Latex Blend (1 : 1)

Parameters	Values
Dispersed phase volume fraction (ν)	0.53, 0.47[a]
Matrix Poisson's ratio (υ_m)	0.35, 0.50[b]
Maximum packing fraction (ν_m)	0.73[c]

[a] For PMMA matrix and for PBA matrix, respectively (see Table II).
[b] For PMMA matrix and for PBA matrix, respectively.[25,26,30]
[c] Maximum packing fraction for monodispersed spherical particles.[25,29]

of ν_m, the maximum packing fraction of the dispersed phase; and α is a function of υ_m, the Poisson ratio of the matrix; subscript m denotes the matrix; subscript i denotes the inclusions.

Based on Dickie's model[24–26] and the experimental moduli of the PBA and PMMA homopolymer latexes (Fig. 4), we calculated the G' and tan δ values of the PBA and PMMA latex blend (1 : 1 w/w). (See Table II for volume fraction of each polymer in the blend.) These calculations were performed under the assumption that the matrix Poisson's ratio (υ_m) is constant at all temperatures[25] and assuming additive volumes of the polymers. The dispersed phase volume fraction (ν) was estimated based on the volume fractions of the polymers in the latex (Table II; assuming that the domains are simply PBA or PMMA homopolymers). Table IV lists the parameters required for these calculations. Figure 5 presents the G'–temperature (top) and tan δ–temperature (bottom) curves of the PBA and PMMA homopolymers (used in the calculations) and the calculated curves for the PBA/PMMA blend, assuming either PMMA or PBA as the continuous phase [Fig. 5(A) and (B), respectively], and our experimental data [Fig. 5(C)].

From Figure 5 (top), a good agreement between the calculated and experimental values for G' is observed when we assume simple PBA inclusions in a PMMA matrix [Fig. 5(A)]. In contrast, considering PBA as the matrix [Fig. 5(B)] leads to a calculated curve completely different from the experimental one. However, assuming a PMMA matrix [Fig. 5(A)], the calculated G' values in the temperature range between the T_g's of PBA and PMMA are higher than the experimental values. The difference between the calculated [Fig. 5(A)] and the measured G' [Fig. 5(C)] curves suggests that the assumption that the dispersed phase consist only of PBA is not valid. Obviously, PBA forms a co-continuous phase within the PMMA matrix. Because of this interconnection, the apparent dispersed phase volume fraction in the film would be higher than the volume fraction of PBA in the original latex (used for the calculation).[24–27,29–32] This arrangement would lead to a material with a lower rigidity than expected from simple PBA domains at the same PBA/PMMA ratio.

Figure 5 (bottom) shows that, considering the experimental errors, the locations of the blend's tan δ peaks are correctly predicted from the calcu-

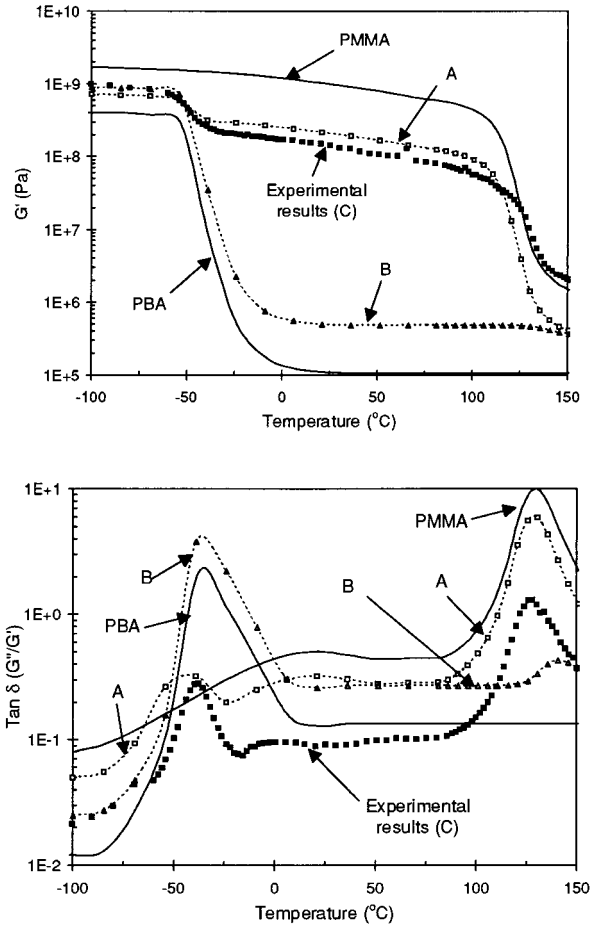

Figure 5 G' (top) and tan δ (bottom) of PBA and PMMA homopolymers (solid lines), and PBA/PMMA homopolymer blend (0.5/0.5 w/w). (A) Values calculated assuming PBA domains in a PMMA matrix. (B) Values calculated assuming PMMA domains in a PBA matrix. (C) Experimentally measured values. Some tan δ curves were shifted vertically by multiplying the values by 4, 2, and 6 [for (A), (B), and PMMA homopolymer, respectively]. (See Table II for polymer compositions in the blend.)

lated values of G' and G'' when a PMMA matrix is assumed [Fig. 5(A)] (-47 ± 3 and 137 ± 3°C experimental, and -43 and 129°C predicted). Nevertheless, the height of the measured PBA peak is higher, while that of the PMMA peak is lower than the calculated values (0.27 ± 0.01 vs. 0.08 for PBA, 1.34 vs. 1.50 for PMMA). This peak height difference also supports the existence of the interconnected PBA domains.[24–26,30,32] (A detailed explanation for the interconnected PBA domains is given in the last section of this paper.) Overall, Figure 5 shows that the choice of parameters in Table IV, and Dickie's equations[24–26] are suitable to help interpret the DMA data for the composite latexes prepared under the current conditions.

Composite Samples

In the last series of experiments, DMA is used for the comparison of films obtained from the composite PBA/PMMA latexes. (See Table II for polymer compositions of these latexes.) The G'–temperature curves in Figure 6 (top) show that all the composite samples behave similarly to the blends, i.e., having two transitions corresponding to the T_g's of the homopolymers. (The curves were vertically shifted for easier identification of the transitions.) These transitions correspond to the phase separation of PBA and PMMA within the composite particles. Additionally, the G' data between the two transitions are parallel to that of the PBA/PMMA homopolymer latex blend, which indicate that, as in the blend, composite latex polymers form films which consist of PBA domains in a PMMA matrix. However, Figure 6 (bottom) shows that although the compositions of all these samples are similar, their G' curves are different. The values of G' in the region between the PBA and PMMA transitions are the lowest for the homopolymer blend. For the case of composite latexes prepared from PBA incorporating macromonomer seed, the values increase with the amount of macromonomer (macromonomer/BA weight ratio) in the seed latexes. However, the values of G' are the highest when the composite latex was prepared from the PBA homopolymer seed particles (BM0). The difference in the G' value reflects the difference in the volume fraction of the dispersed phase in the films.[24–26]

Previously, Cavaille et al. used a parameter relating modulus of films in their relaxed and unrelaxed states to explain the interactions between inclusions and matrix in films prepared from polystyrene and PBA latexes.[29] In the following section, a similar parameter, the change in the modulus before and after the T_g of PBA (G'_{20}/G'_{-100}, G' at 20°C divided by G' at -100°C), is used to approximate the volume fractions of the films' dispersed phase (ν). Table V lists the measured values for G'_{20}/G'_{-100} and for the PBA tan δ peak maxima. (These values represent the averages from up to six specimens per sample.) Apparently, the samples with the higher G'_{20}/G'_{-100} values possess the lower values for the PBA tan δ peak maxima; these values correspond with the lower volume fractions of the dispersed phase in the specimens.

Considering that compression molding of freeze-dried latexes resulted in PBA domains dispersed in a PMMA matrix, one may calculate the values of G', G'', and tan δ at any temperature for PBA/PMMA systems of given polymer compositions. The calculation is based on (1) Dickie's equations,[24–26] (2) the moduli of PBA and PMMA homopolymers (Fig. 4), and (3) parameters listed in Table IV.

In Figure 7, G'_{20}/G'_{-100} values of the PBA/PMMA system calculated based on the assumptions in the above paragraph are plotted vs. volume fraction of the dispersed phase in the system (ν). This plot represents the model-predicted G'_{20}/G'_{-100} values for simple PBA domains (i.e., no PMMA inside these domains) dispersed in a PMMA matrix at different polymer composition. The experimental G'_{20}/G'_{-100} values for the 1 : 1 blend and all the composite samples (Table V) are also plotted as straight lines across the same figure.

From Figure 7, we estimated the values of the film dispersed phase volume fraction (ν) for each sample by determining where the corresponding experimental G'_{20}/G'_{-100} value intersects the model curve. Table VI lists the values for the following: volume fractions of PBA (A) and of the seed polymer (i.e., PBA plus macromonomer) (B) in the composite latexes; the model-predicted volume fraction of the dispersed phase in the compression-molded film (ν) (based on the experimental values of G'_{20}/G'_{-100} (Table V); and ΔV, the difference between columns A and ν. The percentage of the volume of the interfacial polymer based on the PBA phase was also calculated and was reported in the same table. Figure 8 shows schematic diagrams of PBA and PMMA phases in the films prepared from homopolymer latex blend and those prepared from the composite latexes.

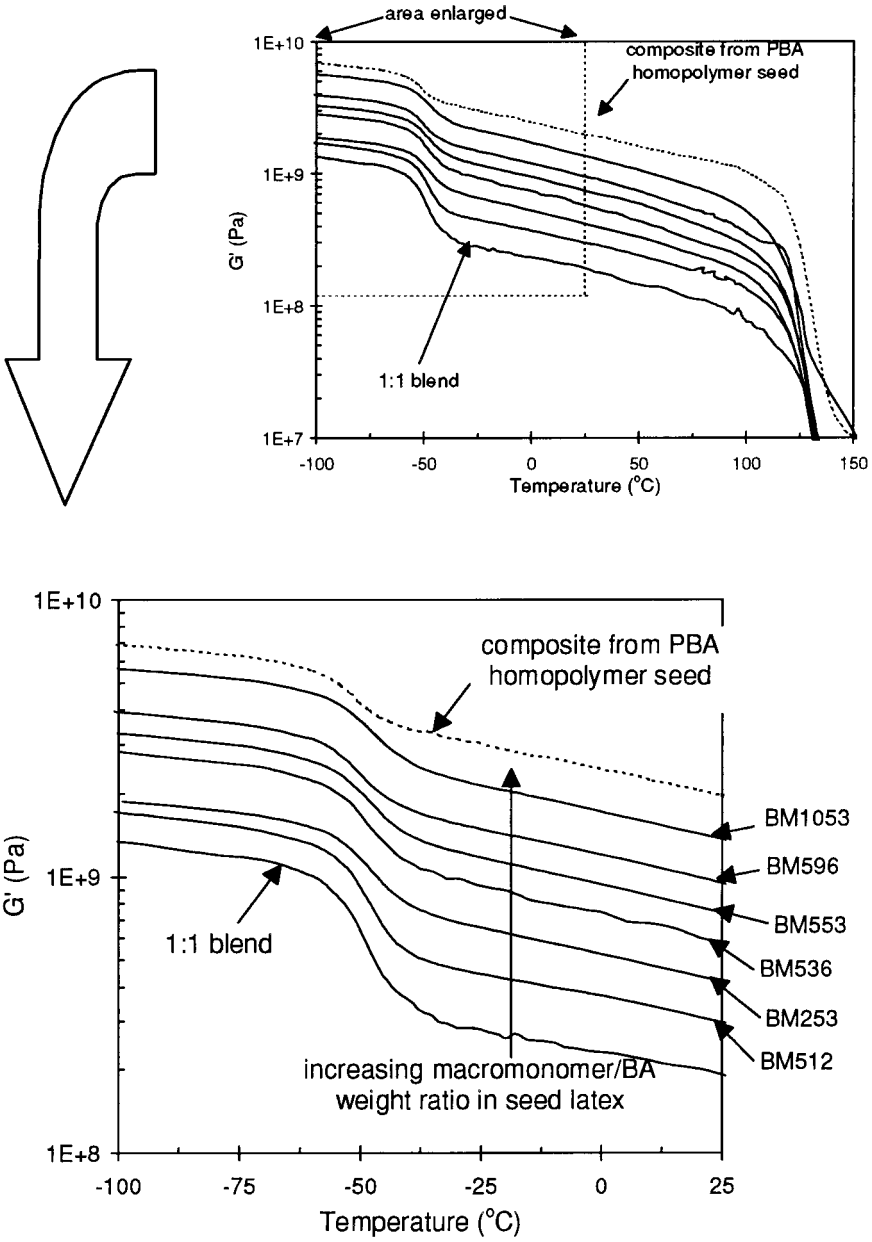

Figure 6 Temperature dependence of G' for films prepared from PBA/PMMA homopolymer blend (0.5/0.5 w/w PBA/PMMA) or composite polymer latexes (seed polymers/MMA in composite latex recipe = 1 : 1 w/w) showing the influence of seed latex compositions. (The curves were shifted vertically by multiplying the G' values by 1.00, 1.75, 1.25, 1.80, 4.00, 2.00, and 4.50, respectively, for the blend, BM512, BM253, BM536, BM553, BM596, BM1053, and BM0.) See Table II for detail of the latexes.

The numbers in Table VI show that the dispersed phase volume fraction in the film made from the PBA/PMMA homopolymer latex blend (0.670) is much higher than the volume fraction of PBA in the original latex blend (0.530). Since the dispersed phase is essentially PBA homopolymer, this unexpectedly high volume fractions of the dispersed phase possibly arise from the interconnection of the PBA domains.[24–26,29–32] In the melt state during the compression molding, individual PBA particles in the blend randomly come into contact with each other. (The high mobility of unattached PBA particles was already discussed earlier in the film-forming experiment.) This pro-

Table V Measured Values of G'_{20}/G'_{-100} and PBA Tan δ Peak Maxima[a]

Sample Name	Macromonomer in Seed Latex: M_w (g/mol)	Macromonomer/BA: mol/mol	Macromonomer/BA: w/w	G'_{20}/G'_{-100}	PBA Tan δ Peak Maxima
Blend	homopolymer blend (1 : 1)			0.122 ± 0.022	0.265 ± 0.013
BM0	prepared from PBA homopolymer seed			0.294 ± 0.014	0.119 ± 0.005
BM512	1260	0.127	1.25	0.168 ± 0.043	0.193 ± 0.003
BM253	5320	0.046	2.04	0.234 ± 0.003	0.135 ± 0.005
BM536	3640	0.127	3.61	0.234 ± 0.024	0.135 ± 0.009
BM553	5320	0.127	5.26	0.242 ± 0.005	0.139 ± 0.005
BM596	9640	0.127	9.53	0.259 ± 0.012	0.120 ± 0.002
BM1053	5320	0.267	11.10	0.249 ± 0.005	0.114 ± 0.005

[a] Experimentally measured and averaged from up to six specimens per sample.

cess enables the existence of small PMMA inclusions within the PBA dispersed phase. This arrangement makes the volume fraction of the dispersed phase in the film higher than the actual volume of PBA in the latex. This film morphology also explains the difference in the measured modulus and the values calculated by Dickie's model shown in Figure 5.

In spite of their similar composition (same volume fraction of PBA in the original latex; see Table VI), the volume fraction of the dispersed phase in a film derived from the composite latex prepared from the PBA homopolymer seed (BM0, 0.535) is much lower than in the one derived from the 1 : 1 homopolymer blend (0.670). The only difference between the blend and this composite sample is that, unlike individual PBA particles in the blend, the PBA phase in the composite particles is attached to the PMMA shell. As already noticed from the film-forming experiment, this attachment slows the migration and diffusion of the PBA chains. The resulting PBA domains are thus smaller and more discrete by the PMMA phase (minimum or no interconnection of PBA domains). The film morphology shown in Figure 8(B) for composite latex prepared from the PBA homopolymer seed also corresponds to the dispersed phase volume fraction in the film being almost the same as the PBA fraction in the original composite latex ($\Delta V = 0.005$). Also, a much higher dispersed phase tan δ peak maximum was recorded (Table V) in the blend (0.265) compared to the one in the composite samples (0.119). (Tan δ peak maximum is related to the dispersed phase volume fraction.)[24–26,30,31]

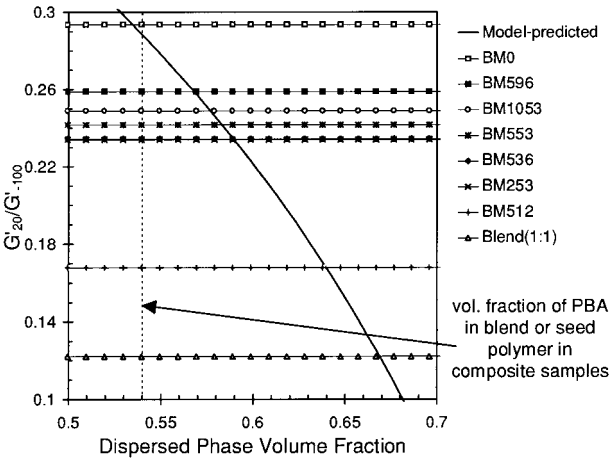

Figure 7 G'_{20}/G'_{-100} for experimental 1 : 1 PBA/PMMA homopolymer latex blend and PBA/PMMA composite latex polymers, and G'_{20}/G'_{-100} versus the dispersed phase volume fraction calculated based on Dickie's model. The G'_{20}/G'_{-100} values for the 1 : 1 blend and all the composite samples are plotted as straight lines across the figure. See Table II for the descriptions of these samples.

Although the volume fractions of seed polymers (i.e., PBA and macromonomer) in all composite latex samples are nearly the same (between 0.528 and 0.530; Table VI), the estimated dispersed phase volume fractions in these films are quite different. However, all the composite films show volume fractions of the dispersed phase higher than the PBA fraction in the original composite latexes (ΔV between 0.071 and 0.117).

For the composite samples prepared from the PBA seed latexes incorporating the lowest molecular weight PMMA macromonomer (BM512), the volume fraction of the dispersed phase appears

Table VI Volume Fractions of Different Phases in the Latexes and in the Compression Molded Films[a]

	Volume Fractions				
	Latex		Film		
Sample Name	(A) PBA	(B) Seed	(ν) Film Dispersed Phase	ΔV (ν-A)	% Interfacial Polymer (Based on PBA)
Blend	0.530	0.530	0.670	0.140	–[b]
BM0	0.530	0.530	0.535	0.005	1.00
BM512	0.523	0.529	0.640	0.117	–[b]
BM253	0.519	0.529	0.590	0.071	13.68
BM536	0.512	0.529	0.590	0.078	15.23
BM553	0.504	0.529	0.583	0.079	15.67
BM596	0.485	0.528	0.569	0.084	17.32
BM1053	0.478	0.528	0.578	0.100	20.92

[a] See Table V for sample compositions and measurement values of G'_{20}/G'_{-100} and tan δ maxima.
[b] Cannot be determined by this method because of the interconnected domains (PMMA inside the PBA dispersed phase).

similar to that of the blend (0.640 and 0.670). For this particular sample, particle agglomeration and interconnected PBA domains [Fig. 8(A)] are anticipated because of the multiphase morphology of the particles [Fig. 3(A)] and the higher mobility of the rubbery phase (T_g of this macromonomer is lower than room temperature,[20] and the latex is film-forming at room temperature). This film morphology is also responsible for the tan δ peak maximum being relatively high (0.193; Table V).

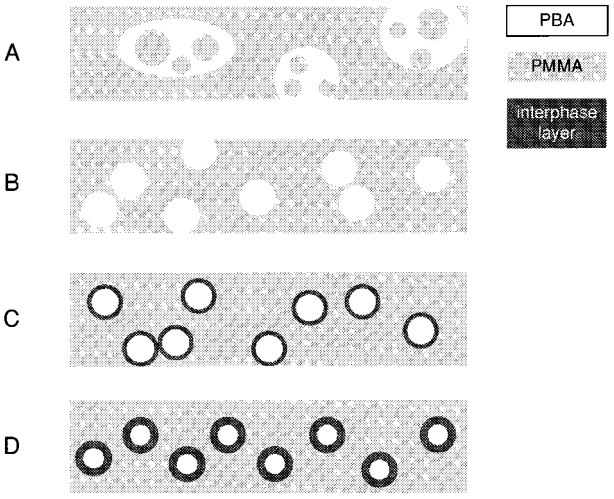

Figure 8 Schematic representations of compression-molded films derived from (A) showing interconnected PBA domains in PMMA matrix (blend or BM512), (B) PBA/PMMA composite latex prepared from PBA homopolymer seed (BM0, showing individual PBA domains), (C) PBA/PMMA composite latex prepared from PBA incorporating macromonomer seed (low macromonomer content), and (D) PBA/PMMA composite latex prepared from PBA incorporating macromonomer seed (high macromonomer content).

For all other composite samples, the film dispersed phase volume fractions (Table VI) and the tan δ peak maxima (Table V) decrease with decreasing latex PBA volume fraction (or the increase in the latex macromonomer content). The difference between the latex's PBA volume fraction and the film's dispersed phase volume fraction ΔV increases with the macromonomer content (Table VI). Based on the DMA results of BM0, minimal domain interconnection occurs in films prepared from all the other composite latexes. Thus, ΔV may only be explained by the presence of an interphase zone between PBA and PMMA in the composite sample when macromonomer is present in the seed particles.[30,32]

Previously, using ^{13}C NMR, Nelliappan et al.[33,34] already showed that an interphase layer exists between the PBA core and PMMA shell of the composite latex particles. They also reported an increase in the thickness of this layer when a BA/PMMA-macromonomer copolymer was used as seed latex. For the latexes prepared under the present conditions, we already showed that macromonomer side-chains of the BA/PMMA-macromonomer graft copolymers partition close to the seed particles–water interface. The partition of

the macromonomer results in a lower interfacial tension between seed particles and water in the seed latexes.[17,19] Subsequently, in the composite latexes, the graft copolymers on the seed particles' surface lower the interfacial tension between seed particles and the newly formed shell. The low interfacial tension leads to composite particles with more uniform coverage of the core particles by the shell polymer (Figs. 2 and 3).

According to the above data, in the composite films, the macromonomer side-chains of the graft copolymers partition close to the seed particle/PMMA interface. This arrangement possibly allows a higher fraction of the rubbery inclusions to integrate extensively into the PMMA matrix and compatibilize these two polymer phases, forming an interphase layer. The difference between the PBA volume fraction in the original latexes and the dispersed phase volume fraction in the films (ΔV) is indicative of the volume of this interphase layer. ΔV correlates well with the increase in the amount of incorporated macromonomer (weight ratio of macromonomer to BA) in the seed latex. The higher volume fractions of the dispersed phase in the films compared with the volume fraction of the seed polymers in the composite latexes could be explained by two possible reasons: (1) the PBA volume in the sample is lower than the number calculated based on weight of BA used to prepare the original seed latex because a large fraction of the PBA chains is copolymerized with macromonomer and become a part of the interphase layer, and (2) the model used for the determination of the dispersed phase volume fraction does not account for the presence of the interphase zone but assumes simple PBA domains in the PMMA matrix.

In conclusion, DMA results show that, by using PBA seed incorporating PMMA macromonomer to prepare the composite latexes, the PBA homopolymer volume fraction decreases, and the volume fraction of the interphase region between the two polymer phases increases. By increasing the number of MMA units in the BA/PMMA-macromonomer graft copolymer (either by increasing the mole ratio of macromonomer to BA or by increasing the molecular weights of the macromonomers), the volume of the interfacial layer increases. Both the decrease in the rubber phase volume fraction and the higher volume of the interphase layer correlate with the better compatibility of PBA and PMMA in the composite particles when macromonomer is present in the seed particles (as previously observed from our TEM micrographs and ^{13}C NMR results[33,34]).

CONCLUSIONS

Composite latex particles containing 1 : 1 (w/w) PBA and PMMA were prepared by polymerizing MMA in the presence of PBA seed latex particles. Compatibilizing agents (BA/PMMA macromonomer copolymers) were already incorporated into the PBA seed latexes *in situ* (during their preparation). The observed increase in the size averages and narrowing of the size distributions of the composite latex particles compared with those of the corresponding seed particles show that the second-stage MMA monomer is completely polymerized onto the seed particles.

For morphological characterization of the composite particles, TEM with the preferential staining method was used. The degree of phase separation between the two polymers in the composite particles is affected by the amount of macromonomers used in the seed latex preparation (i.e., mole ratio of macromonomer to BA and molecular weight of the macromonomers). The observed morphologies show quite a good agreement with the decrease in the polymer$_1$/aqueous phase interfacial tensions observed when PMMA macromonomer was incorporated into the PBA seed particles.[17] These results indicate that the decrease in polymer/polymer interfacial tension enhance the seed coverage by the shell polymer. Thus, interfacial tension is considered one of the main parameters controlling particle morphology in composite latexes.

The inability of the composite latexes to form film at room temperature suggests the reduced mobility of the PBA phase when attached to the PMMA shell. The dynamic mechanical analysis interpreted according to Dickie's model for phase-separated polymer blends[24–26] show a decrease in the PBA volume fraction and an increase in the volume fraction of the interface layer when the BA/PMMA macromonomer copolymer seed particles were used. These results also agree with the observed particle morphology and Nelliappan's ^{13}C-NMR studies on PBA core-PMMA shell latexes.[33,34]

REFERENCES

1. M. Okubo, Y. Katsuta, and Y. Matsumoto, *J. Polym. Sci., Polym. Lett. Ed.,* **18,** 481 (1980).

2. M. Okubo, *Makromol. Chem., Macromol. Symp.,* **35,** 307 (1990).
3. A. Rudin, *Makromol. Symp.,* **92,** 53 (1995).
4. J. Cho and K. W. Lee, *J. Appl. Polym. Sci.,* **30,** 1903 (1985).
5. S. Lee and A. Rudin, *Makromol. Chem., Rapid Commun.,* **10,** 655 (1989).
6. G. A. Vandezande and A. Rudin, *J. Coating Tech.,* **66,** 99 (1994).
7. M. Okubo, Y. Katsuta, and T. Matsumoto, *J. Polym. Sci., Polym. Lett. Ed.,* **20,** 45 (1982).
8. T. I. Min, A. Klein, M. S. El-Aasser, and J. W. Vanderhoff, *J. Polym. Sci., Polym. Chem. Ed.,* **21,** 2845 (1983).
9. V. L. Dimonie, M. S. El-Aasser, A. Klein, and J. W. Vanderhoff, *J. Polym. Sci., Polym. Chem. Ed.,* **22,** 2197 (1984).
10. S. Eckersley and A. Rudin, *J. Appl. Polym. Sci.,* **53,** 1139 (1994).
11. S. Torza and S. G. Mason, *J. Colloid Interf. Sci.,* **33,** 67 (1970).
12. D. C. Sundberg, A. P. Casassa, J. Pantazopoulos, M. R. Muscato, B. Kronberg, and J. Berg, *J. Appl. Polym. Sci.,* **41,** 1425 (1990).
13. V. L. Dimonie, M. S. El-Aasser, and J. W. Vanderhoff, *Polym. Mat. Sci. Eng.,* **58,** 821 (1988).
14. Y. C. Chen, V. L. Dimonie, and M. S. El-Aasser, *J. Appl. Polym. Sci.,* **41,** 1049 (1991).
15. Y. C. Chen, V. L. Dimonie, and M. S. El-Aasser, *Macromolecules,* **24,** 3779 (1991).
16. Y. C. Chen, V. L. Dimonie, and M. S. El-Aasser, *J. Appl. Polym. Sci.,* **45,** 487 (1992).
17. P. Rajatapiti, V. L. Dimonie, and M. S. El-Aasser, *J. Macromol. Sci., Chem.,* **32,** 1445 (1995).
18. W. Chotirotsukon, M.S. Thesis, Lehigh University, 1991.
19. P. Rajatapiti, V. L. Dimonie, and M. S. El-Aasser, *J. Appl. Polym. Sci.,* **61,** 891 (1996).
20. P. Rajatapiti, Ph.D. Dissertation, Lehigh University, 1996.
21. J. Brandrup and E. H. Immergut, Eds., *Polymer Handbook,* 3rd ed., Wiley-Interscience, New York, 1989, p. VI/209.
22. M. J. Devon, J. L. Gardon, G. Roberts, and A. Rudin, *J. Appl. Polym. Sci.,* **39,** 2119 (1990).
23. M. Hidalgo, J. Y. Cavaille, J. Guillot, C. Pichot, R. Rios, and R. Vassoille, *Colloid Polym. Sci.,* **270,** 1208 (1992).
24. R. A. Dickie, M. F. Cheung, and S. Newman, *J. Appl. Polym. Sci.,* **17,** 65 (1973).
25. R. A. Dickie, *J. Appl. Polym. Sci.,* **17,** 45 (1973).
26. R. A. Dickie and M. F. Cheung, *J. Appl. Polym. Sci.,* **17,** 79 (1973).
27. G. Canche-Escamilla, E. Mendizabal, M. J. Hernandez-Patino, S. M. Arce-Romero, and V. M. Gonzalez-Romero, *J. Appl. Polym. Sci.,* **56,** 793 (1995).
28. K. M. O'Conner and S. L. Tsaur, *J. Appl. Polym. Sci.,* **33,** 2007 (1987).
29. J. Y. Cavaille, R. Vassoille, G. Thollet, L. Rios, and C. Pichot, *Colloid Polym. Sci.,* **269,** 248 (1991).
30. C. Jourdan, J. Y. Cavaille, and J. Perez, *Polym. Eng. Sci.,* **28,** 3218 (1988).
31. J. Y. Cavaille, C. Jourdan, X. Z. Kong, J. Perez, and C. Pichot, *Polymer,* **27,** 693 (1986).
32. C. Pichot, X. Z. Kong, J. Guillot, and J. Y. Cavaille, *Polym. Mat. Sci. Eng.,* **64,** 276 (1991).
33. V. Nelliappan, M. S. El-Aasser, A. Klein, E. S. Daniels, and J. E. Roberts, *J. Polym. Sci., Polym. Chem. Ed.,* **34,** 3173 (1996).
34. V. Nelliappan, M. S. El-Aasser, A. Klein, E. S. Daniels, and J. E. Roberts, *J. Polym. Sci., Polym. Chem. Ed.,* **34,** 3183 (1996).

Received May 22, 1996
Accepted June 25, 1996